Analysis of chemical perturbation of stratospheric air parcel along the trajectory during the Arctic winter of 1996/1997 using ILAS data

Yukio Terao*[a], H. L. Tanaka[a], Tetsuzo Yasunari[a], and Yasuhiro Sasano[b]

[a] Institute of Geoscience, University of Tsukuba, Ibaraki 305-8571, Japan
[b] National Institute for Environmental Studies, Ibaraki 305-0053, Japan

ABSTRACT

Reanalysis was made for quantitative chemical ozone loss rates in the Arctic stratospheric vortex by using ozone profile data (Version 5.10) obtained with the Improved Limb Atmospheric Spectrometer (ILAS) for the spring of 1997. The analysis method is based on the Match technique. In this study we calculated additional trajectories and set very strict criteria to identify a double-sounded air mass more reliably. The result shows that the integrated ozone loss during February and Match was 1.9 ppmv at 492–450 K levels (about 60 % losses) and the column ozone loss during two months was 94 DU. The ozone loss rate of the present study was larger than that of the sonde-Match analysis.

Keywords: Arctic, ILAS, Lagrangian method, ozone layer, ozone loss, satellite measurement, stratosphere, trajectory

1. INTRODUCTION

Separating ozone changes due to chemistry from those due to dynamics is a very important subject for better understanding of the polar stratospheric ozone depletion. However, that is a difficult task and requires careful treatments. One method to solve this difficulty is known as "Match".[1–3] They used pairs of ozonesonde profiles which were obtained at separated locations but were identified through Lagrangian trajectories so that they observed the same air mass. By this approach, dynamical effects in ozone changes can be neglected and only chemical changes remain.

We applied a similar technique to ozone profile data obtained with a satellite-borne sensor, Improved Limb Atmospheric Spectrometer (ILAS),[4] and presented preliminary estimates of the ozone loss rates and amounts during the Arctic spring of 1997[5] and the nitric acid change rates observed at the same time.[6] However, there are concerns about the conservation of air masses in our satellite-Match analysis since satellite sensor data have a relatively low vertical resolution and a larger sampling air mass volume than ozonesonde data. In order to conquest the disadvantages in satellite sensor data, we set much stricter criteria than the sonde-Match to identify double-sounded air masses more reliably.

This paper presents the methods for a multiple trajectory analysis to select double-sounded air masses and results of reanalysis on the ozone loss rates and amounts using the newest products of ILAS (Version 5.10). A relationship between ozone loss and temperature history of the air masses and dependence of ozone loss rates on the criteria for sampling data are also discussed.

2. DATA AND ANALYSIS METHOD

2.1. Data

ILAS is a sensor that is based on the solar occultation technique and provides vertical profiles of gas species (ozone, nitric acid, nitrogen dioxide, methane, nitrous oxide, and water vapor) by infrared spectrometry and aerosol extinction coefficient by visible.[4] The present analysis uses ILAS Version 5.10 data for ozone mixing ratio profiles. The UKMO assimilation data (a grid of 2.5° (latitude) × 3.75° (longitude) × 22 UARS standard pressure levels from 1,000 hPa to 0.316 hPa, 1200 UT) are used for meteorological analyses and trajectory calculations.

*Correspondence: E-mail: terao@luft.geo.tsukuba.ac.jp; Telephone: 81 298 53 6139; Fax: 81 298 51 9764

Optical Remote Sensing of the Atmosphere and Clouds II, Yasuhiro Sasano, Jinxue Wang, Tadahiro Hayasaka, Editors, Proceedings of SPIE Vol. 4150 (2001) © 2001 SPIE · 0277-786X/01/$15.00

Table 1. Trajectory calculation levels. * is three months mean during February, March, and April.

Potential temperature (K)	Approximate height (km) *	+0.8 km level (K) *	-0.8 km level (K) *
375	13.6	387.8	361.9
400	15.0	413.6	386.6
425	16.4	440.1	410.4
450	17.7	466.7	433.9
475	18.9	493.1	457.4
500	19.9	519.3	481.2
525	20.9	545.5	505.1
550	22.2	571.8	529.0
600	23.6	624.6	576.4

2.2. Trajectory analysis

An air parcel that the ILAS sounded twice at different locations and at different times (a double-sounded air parcel; match) are searched from the ILAS data set with 10-day forward isentropic trajectories, and a change of mixing ratio of each gas species is calculated from the two profiles for the air parcel considering the diabatic descent effects.

The program for trajectory analysis used in this study is on isentropic Lagrangian model which was supplied by UKMO. The main specifications of the trajectory model are as follows: The integration in calculating trajectory is done by the cubic Runge-Kutta scheme with one hour interval. The time interpolation and the space interpolation are done linearly with respect to the horizontal direction, and the vertical interpolation is done linearly with respect to the log-P coordinate.

Our previous analysis[5] was based only on a single forward trajectory, which started from each observation point (location #1) for searching a matching observation (location #2), on nine potential temperature levels from 375 K to 550 K with 25 K intervals, and 600 K (Table 1). In the sonde-Match analysis, a single forward trajectory was used for searching a match in 1991/1992 winter[1,2] and additional six forward trajectories around each sonde measurement point were introduced to check accuracy of matches in 1994/1995 winter.[3] Since satellite sensor data have a relatively low vertical resolution (ILAS has a vertical resolution of about 2 km) and larger sampling air mass volume than ozonesonde data, a strict criterion about the conservation of air masses is introduced to identify a double-sounded air mass more reliably in the present study.

First, we calculate a backward trajectory which starts from the location #2. Figure 1 shows an example of a single forward/backward trajectory at 475 K potential temperature surface. In the case of Figure 1, the forward trajectory which starts from the location #1 matches well with the location #2, however the backward trajectory from the location #2 never gets close to the location #1. Such a case should be avoided from the analysis.

Furthermore, we consider a cluster of forward trajectories which start from around the location #1 and a cluster of backward trajectories from around the location #2. The initial volume of the cluster represents a finite sampling air mass volume of ILAS, which is 1.6 km in height and 300 km in distance as a maximum estimation. Figure 2 illustrates a schematic picture of ILAS sampling air mass volume and a corresponding multiple trajectory analysis. We calculate additional four trajectories which start from points separated by ± 150 km along the line of sight on the two surfaces separated by ± 0.8 km in altitude around each ILAS observation point at its tangent height. Figure 3 shows an example of a cluster of forward/backward trajectories. In this case, the location #1 and the location #2 are defined by both forward and backward center trajectories (thick solid curves). As shown in the left hand panel of Figure 3, there are large differences between upper and lower level trajectories, and the locations of the end point of each trajectory are quite different. That can be explained by a large vertical shear in the wind field. Also, as shown in the right hand panel of Figure 3, there are large differences between upper (or lower) two trajectories, which corresponds to a large horizontal shear in the wind field. As such, if multiple four forward/backward trajectories diverge significantly, these trajectories should be considered unreliable.

In total, ten trajectories (a single forward/backward trajectory and a cluster of four forward/backward trajectories) are calculated for each ILAS measurement on each level shown in Table 1. An example shown in Figure 4 indicates

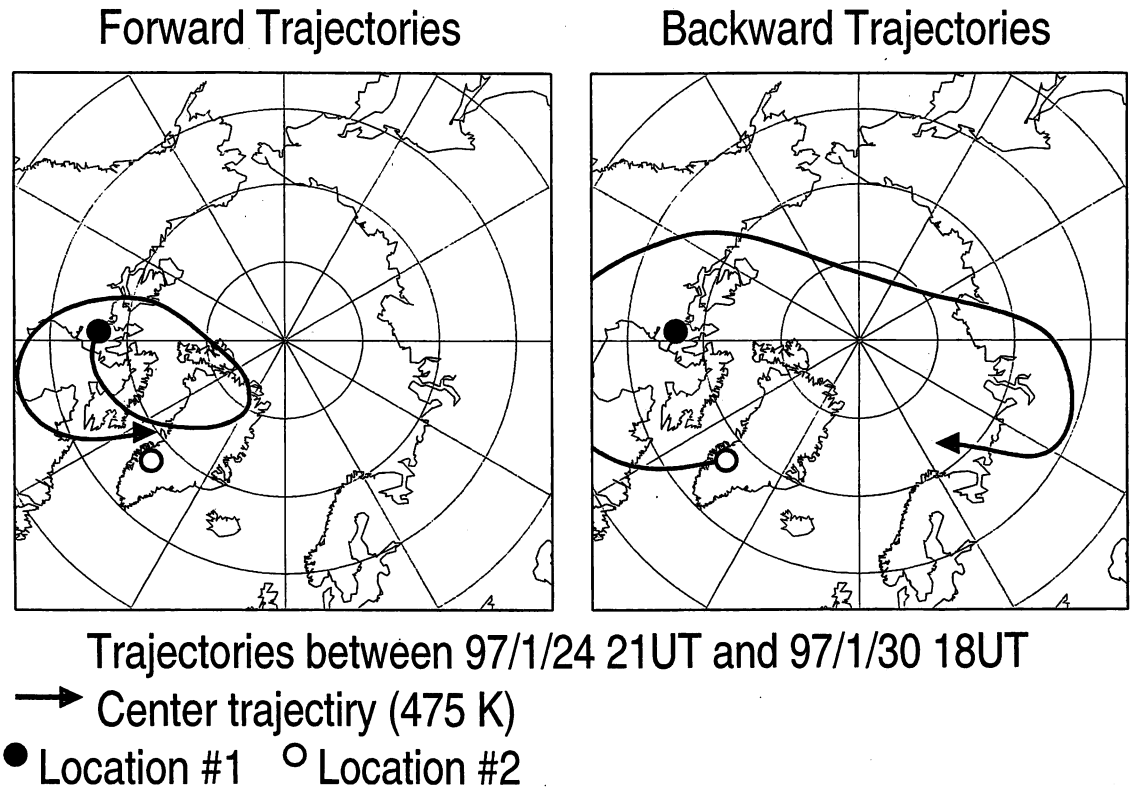

Figure 1. Example of single forward (left) and backward (right) trajectories at 475 K potential temperature surface between January 24 and January 30, 1997. The first ILAS measurement point (location #1) is marked by large solid circle and the second point (location #2) by large open circle.

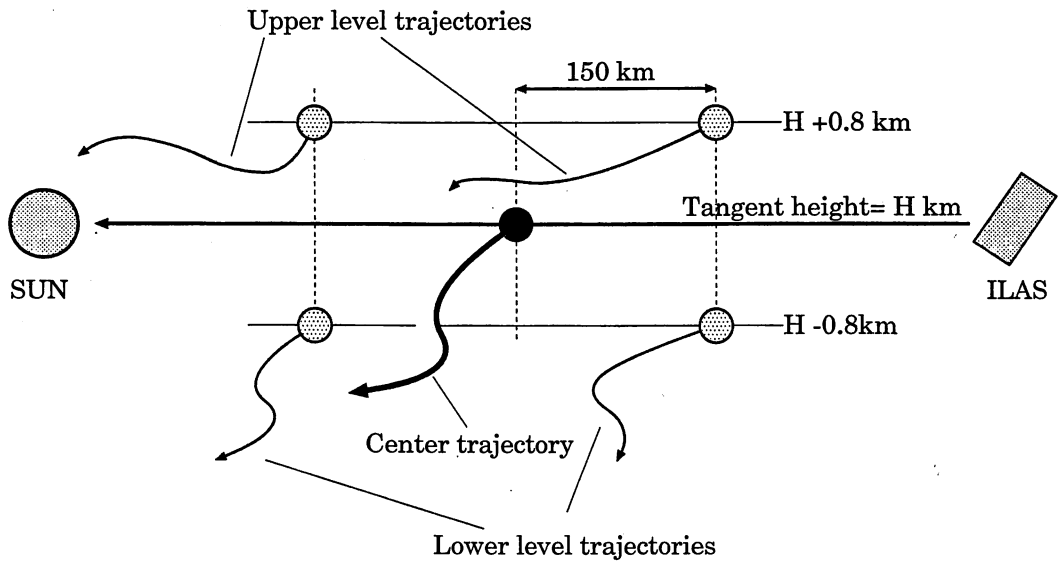

Figure 2. Schematic picture of ILAS sampling air mass volume and a corresponding cluster of trajectories.

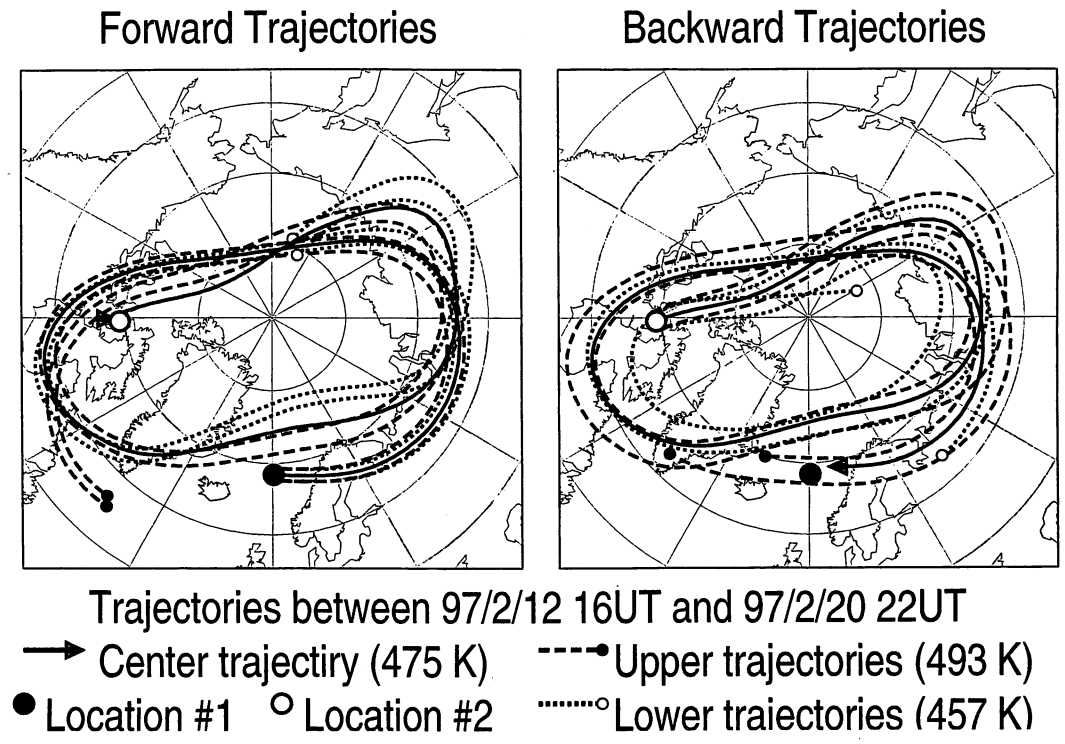

Figure 3. Example of a cluster of forward (left) and backward (right) trajectories during February 12 and February 20, 1997. A thick solid curve with an arrow shows a center trajectory on 475 K potential temperature surface. Dashed and dotted trajectories are on upper levels (493 K) and on lower levels (457 K), and small solid and open circles show the end of each trajectory on upper levels and on lower levels, respectively.

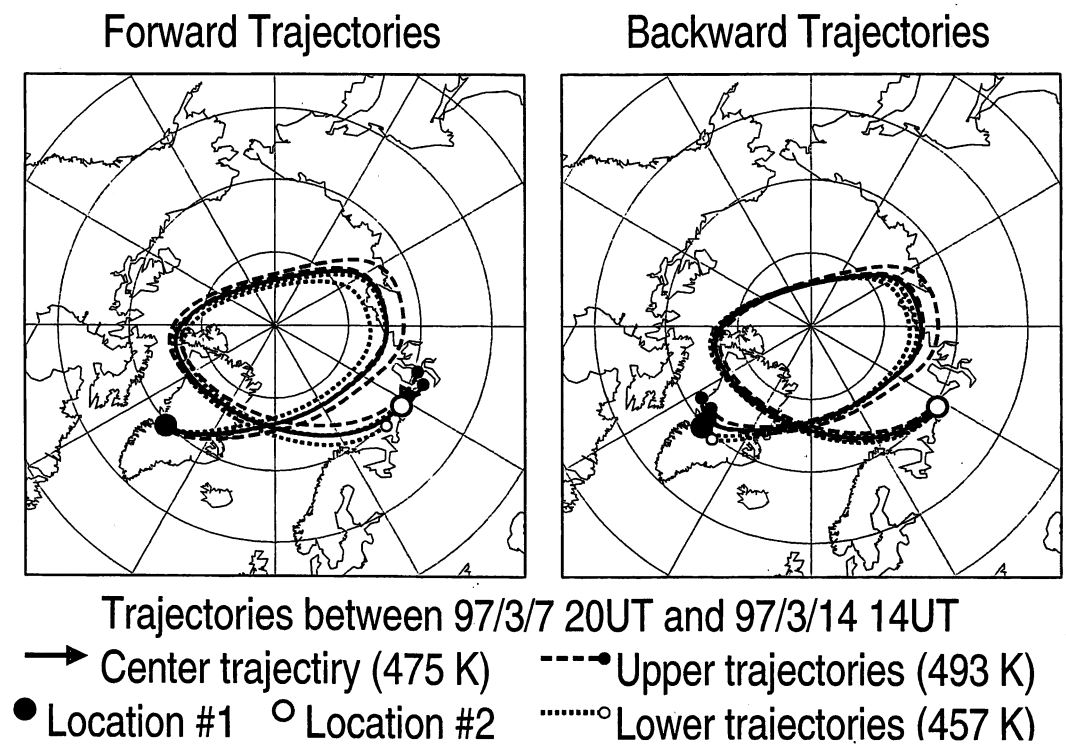

Figure 4. Same as in Figure 3 but during March 7 and March 14, 1997.

that all of the forward and backward trajectories are very compact during seven days, resulting in that we can determine a double-sounded air parcel reliably.

2.3. Selection of a double-sounded air parcel

We set several criteria for selecting double-sounded air parcels.

- Distance (referred as a forward match radius) between the position of location #2 and the central forward trajectory which starts from location #1, which corresponds to the distance between the large open circle and the tip of the thick solid arrow in the left hand panel of Figure 4, should be less than 500 km.
- Distance (referred as a forward cluster radius) between the position of location #2 and all four forward trajectories which start from around location #1, which corresponds to the distance between the large open circle and each small solid or open circle in the left hand panel of Figure 4, should be less than 1600 km.
- The same criteria are applied to the backward trajectory analysis. Thus, a backward match radius should be less than 500 km and a backward cluster radius less than 1600 km.
- Difference between the maximum and the minimum value of potential vorticity along the central forward trajectory, to which a 24-hour running mean was applied, (referred as Δ PV) should be less than 20 %.

These criteria were chosen on the basis of the error analysis similar to that by Ref. 2,3. Figure 5 shows a standard deviation of ozone mixing ratio change as a function of a maximum forward match radius and a backward match radius, in which the ozone change is corrected by an expected ozone change along the trajectory. The expected ozone change was calculated by multiplying the sunlit time along the trajectory with the ozone change rate per sunlit time. The way of determining the ozone change rate by regression analysis is described below. Figure 5 indicates a dependence of a residual ozone change from the regression line, namely, an error, on the distance criterion. If a larger distance criterion is used, the error becomes larger. If a smaller distance is used, the number of matches is too small to calculate ozone change rate statistically meaningful. In this way, 500 km was chosen as the criterion for the present analysis. The criteria of a forward/backward cluster radius and Δ PV were determined in the same manner as the forward/backward match radius.

The search was done only for the matching pairs obtained inside the polar vortex. The poleward edge of the vortex boundary was defined on each day based on a similar method to Ref. 7. In this way the ILAS measurements that were located well inside the polar vortex were selected for further analysis.

Table 2 shows the total number of double-sounded air parcels for corresponding criteria during February and March. If we considered only forward match radius and ΔPV, which was done in Ref. 5, more than a thousand of matches were obtained. When we add the backward match radius criterion, the number of matches reduced to about half. By considering all of the criterion described above, several hundreds matching pairs were identified for each month (row-3 in Table 2). Although these are less than one third of the number in the previous study (row-1 in Table 2), these are enough to statistically calculate a ozone change rate.

Table 2. Total number of double-sounded air parcels between 400 and 600 K potential temperature surfaces for a corresponding criteria during February and March.

	Criteria	Feb	Mar
1	forward match radius $\leq$ 500 km and ΔPV $\leq$20 %	1492	2237
2	1 + backward match radius $\leq$ 500 km	770	902
3	2 + forward and backward cluster radius $\leq$ 1600 km	590	654

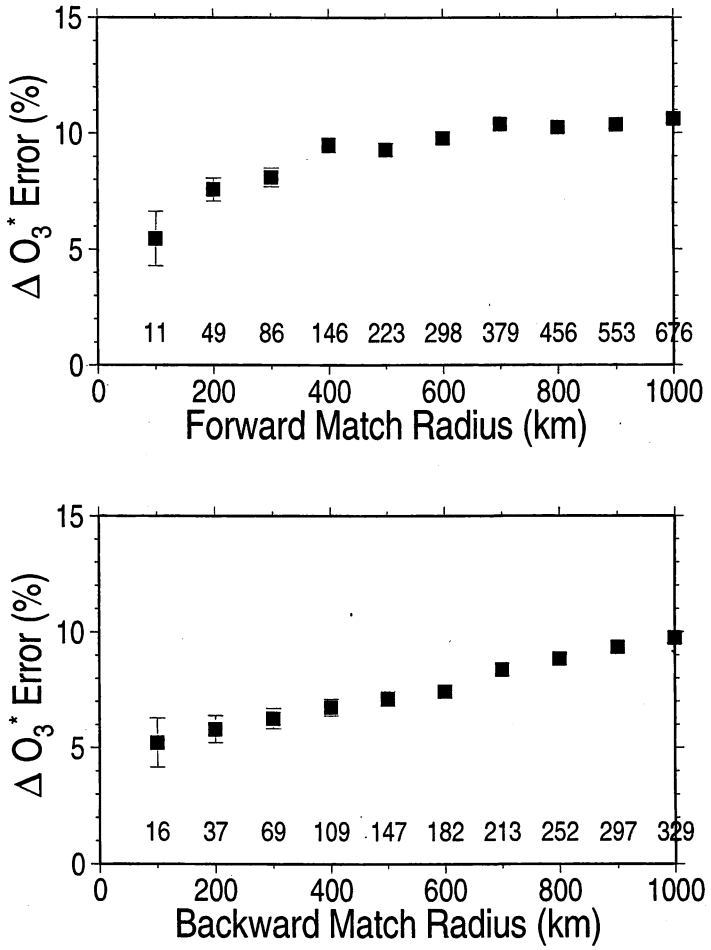

Figure 5. Standard deviation of ozone mixing ratio change which is corrected by the expected ozone loss along the trajectory as a function of a maximum forward match radius (top) and a backward match radius (bottom). The data used here were obtained during day 50 to day 80 on 525 K potential temperature surface. The values plotted near the bottom indicate the number of matches for a corresponding criterion.

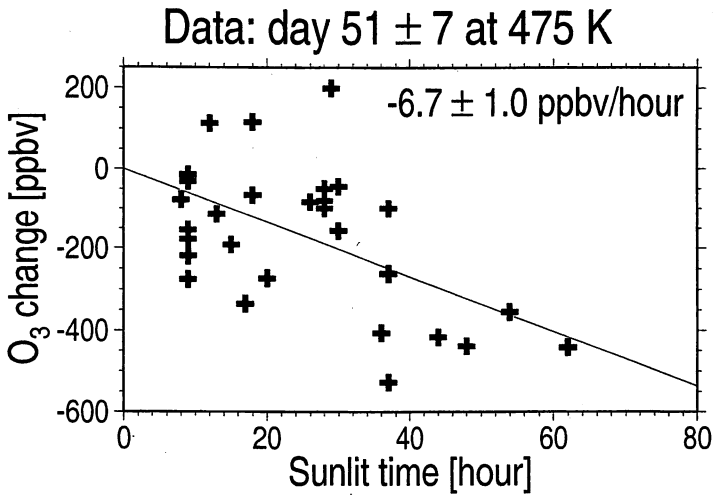

Figure 6. A scatter plot for ozone mixing ratio change of a corresponding matching pair as a function of sunlit time along the trajectory. The data used here were obtained during day 44 to day 58 at 475 K potential temperature surface. A regression coefficient is referred to as an ozone change rate at day 51, which value is -6.7 ± 1.0 ppbv/ sunlit hour.

2.4. Calculation of ozone loss rate

A change in ozone mixing ratio (referred as ΔO_3) is calculated by considering changes in potential temperature by diabatic effects (referred as $\Delta\theta$) as $\Delta O_3 = O_3(\theta+\Delta\theta)_{\text{location\#2}} - O_3(\theta)_{\text{location\#1}}$, where $O_3(\theta)$ means an ozone mixing ratio on θ potential temperature level and the subscript indicates a location of ILAS observation. Thus, the ozone mixing ratio at the location #2 is modified by potential temperature changes due to diabatic cooling during the flight time. The diabatic cooling rates averaged over the polar vortex were taken from Ref. 8. A statistical treatment is applied to the subset of double-sounded air parcels to calculate ozone change rates for each day. Each subset consists of matching pairs that are gathered within seven days before and after each target day. Assuming that ozone changes are linearly proportional to the sunlit time along the trajectory, a proportional coefficient (ozone change rate against sunlit time) is calculated using the least-squares method from each subset of data. Figure 6 shows a scatter plot for ozone mixing ratio change of a corresponding matching pair as a function of sunlit time along the trajectory and an example of calculation of ozone loss rate. The data used in this figure were obtained during day 44 to day 58 at 475 K potential temperature surface, and the regression coefficient is referred to as an ozone change rate at day 51.

3. RESULTS AND DISCUSSION

3.1. Ozone change rate

Figure 7 (a) shows a contour plot of chemical ozone loss rates in ppbv per day as functions of potential temperature and date. These were calculated by multiplying the ozone loss rate in ppbv per hour with the sunlit time (hours) for each day. Ozone losses took place at almost all the altitudes during February and March. Especially, large ozone losses appeared during late-February, where the local maximum ozone loss rate was 50–70 ppbv/day at 450–500 K potential temperature levels. Vertical bars in the figure indicate the region with less statistical significance than 99%. Although some white regions which mean ozone gain appeared in mid-February and mid-March, they have no statistical significance.

Figure 7 (b) shows integrated ozone changes from day 30 to 90 along the potential temperature changes of air parcels which were illustrated by smooth thin curves in (a). Note that the integration were done for the day 57-101 and day 39-101 for the uppermost two levels, respectively. The integrated ozone loss shows its maximum of 1.9 ± 0.1 ppmv on the surface that reached the 450 K level on March 31 from the 492 K level on February 1. This is about 60% of the initial (February 1) ozone concentration.

Furthermore, ozone column change rates are shown in Figure 7 (c), where the local ozone change rates (in number density per day) were integrated from 400 to 600 K. Monthly-mean temperature and pressure profiles inside the

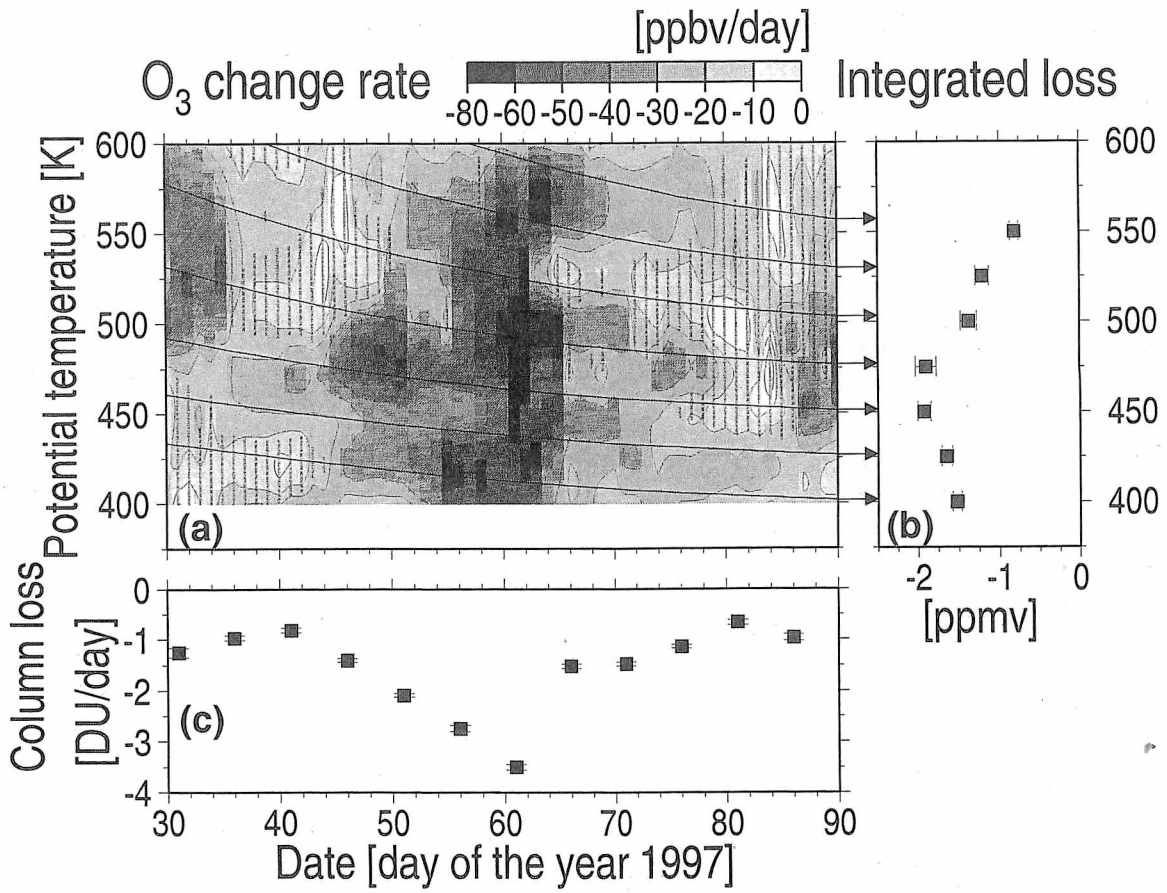

Figure 7. **(a)** Contour plot of ozone change rates (in ppbv per day) as a function of potential temperature and date (day of the year 1997). A contour interval is 10 ppbv/day, and ozone loss regions are shaded. Vertical bars indicate the region with statistical significance less than 99%. Smooth thin curves show potential temperature changes of air parcels (diabatic descent of air masses).[8] **(b)** Integrated ozone changes from January 30 to April 11 (day 30-101) (day 57-101 and day 39-101 for the uppermost two levels, respectively) along the descent curves of air masses as a function of potential temperature. Error bars represent one sigma. **(c)** Ozone column change rates (in DU per day) as a function of date, which were obtained by integrating the local ozone change rates (in number density per day) from 400 to 600 K. Plots were done every five days. Error bars represent one sigma.

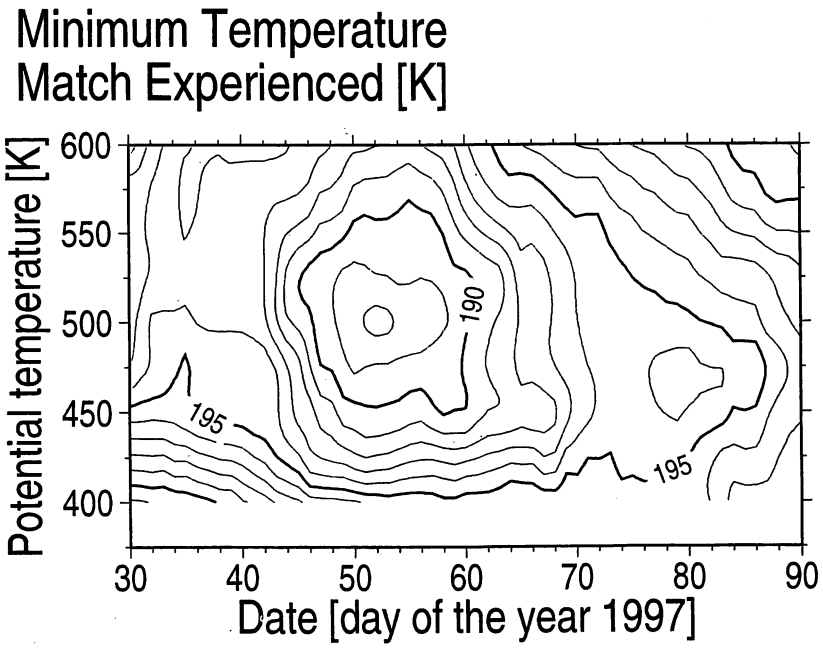

Figure 8. Minimum temperature along a 10-day backward trajectory and a trajectory between location #1 and location #2 for corresponding matching pairs. A contour interval is 1 K.

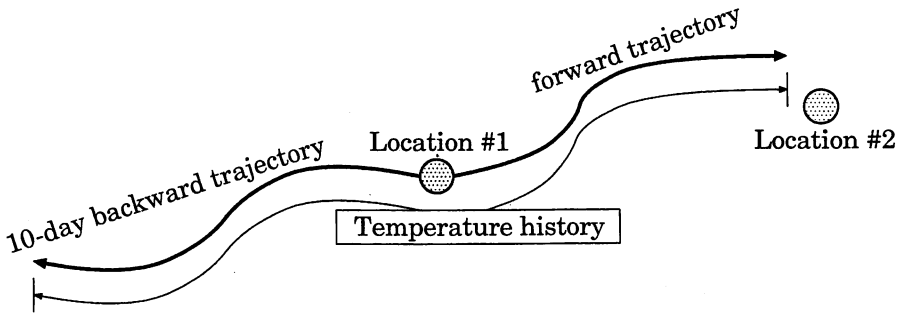

Figure 9. Schematic picture of temperature history analysis.

vortex were used to convert the unit of ozone change rate from mixing ratio to column amount. The column ozone loss during the two months was 94 DU.

3.2. Ozone loss and temperature history along the trajectory

Figure 8 shows the average of the minimum temperature along a 10-day backward trajectory from a location #1 and a trajectory between a location #1 and a location #2 for corresponding matching pairs (see also Figure 9). The minimum temperature was recorded for each double-sounded air parcel and averaged within seven days before and after each target day in the similar way to when calculating the ozone loss rate. The region where the temperature dropped below 195 K low enough to produce NAT-PSCs appeared at almost all altitude in February and early March. In particular, during Days 45–60 and between 450 K and 555 K potential temperature surfaces, the air masses experienced very low temperature below 190 K enough to produce Ice-PSCs. Comparison of the temperature history and the ozone loss rate in Figure 7 (a) suggests a clear relation between them. The very low temperature corresponds to the regions of the large ozone loss.

The ozone loss rate estimated in the present study is larger than that of the sonde-Match during the same period.[9] There are differences not only in the data source (satellite or ozonesonde measurement) or the details of analysis method (e.g. a trajectory calculation tool and a match-criterion) but also in the minimum temperature which each

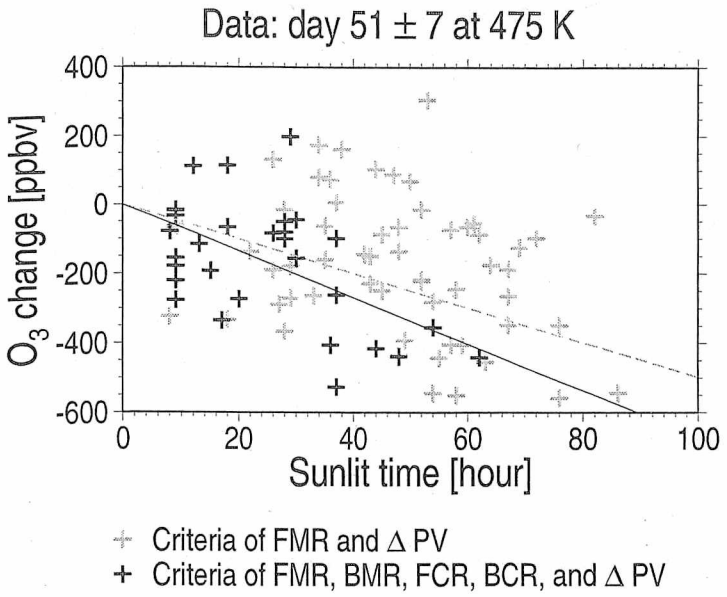

Figure 10. A scatter plot for ozone mixing ratio change of a corresponding matching pair as a function of sunlit time along the trajectory. The data used here were obtained during day 44 to day 58 at 475 K potential temperature surface. Gray crosses plot the data which were selected under the two criteria of forward match radius and Δ PV and a dashed line indicates the ozone change rate derived from gray crosses (-5.0 ± 0.5 ppbv/sunlit hour). Black crosses plot the data which were selected under the all criteria of forward/backward match radius, forward/backward cluster radius, and Δ PV and a solid line indicates the ozone change rate derived from the subset of black crosses (-6.7 ± 1.0 ppbv/sunlit hour).

matching pair may have experienced. The minimum temperature of the present study was 2-3 K lower than that of Ref. 9. This implies that the double-sounded air parcels for our study traveled more inner part of the vortex where the temperature was lower, causing a higher possibility of PSCs existence and a larger ozone loss. Furthermore, most of ILAS observation points were located in the higher latitude region than the ozonesonde stations.

3.3. Dependence of ozone loss rate on match-criteria

The ozone loss rate derived here is also larger than that from our previous study.[5] The differences can be understood mainly because of the following two reasons.

One is the difference in the ILAS product version; Ref. 5 used Version 3.10 and the present study Version 5.10. However, for the ozone products, the differences are relatively small.

Another is the difference in the criteria for selecting double-sounded air parcels. As described above, Ref. 5 used only a single forward trajectory for searching a matching observation, while the present study used ten trajectories and set stricter criteria. In order to assess the dependence of the ozone loss rate on the difference in the match-criteria, we compared ozone change rates which were derived from different match-criteria in Figure 10. The ozone change rate for the corresponding criteria of Ref. 5, in which only two criteria of forward match radius and Δ PV were used, was -5.0 ± 0.5 ppbv/sunlit hour (the dashed gray line in Figure 10). On the other hand, the ozone change rate under the criteria of the present study was larger and -6.7 ± 1.0 ppbv/sunlit hour (the solid black line). By adding the criteria for a backward trajectory and a cluster of trajectories, the data points which give little change in ozone mixing ratio in spite of long sunlit time (gray crosses near the zero line during 40-80 sunlit hour) were filtered out. As a result of this filter-out, the ozone loss rate in the present study was larger than the previous one.

4. CONCLUSION

Quantitative chemical ozone loss rates and amounts in the Arctic stratospheric vortex were calculated by using ILAS newest ozone profile data (Version 5.10) for the spring of 1997. The analysis method is similar to the Match technique.

In order to conquest the disadvantages in satellite sensor data, i.e. low vertical resolution and larger sampling air mass volume, the analysis method was improved and very strict criteria about a conservation of air masses was introduced to identify a double-sounded air mass more reliably. For this purpose, a single forward/backward trajectory and a cluster of four forward/backward trajectories were calculated for each ILAS observation.

The result shows that the local maximum ozone loss rate was 50-70 ppbv/day during late-February at 450–500 K levels. The integrated ozone loss during February and March was 1.9 ppmv at 492–450 K levels and the column ozone loss during the two months was 94 DU. The ozone loss rate of the present study was larger than that of the sonde-Match analysis and our previous study. The former is mainly because the matching air mass in our study traveled over the more inner part of the vortex, and the ILAS observation points were located in the higher latitude region than the ozonesonde observations. The latter is because erroneous double-sounded air masses were filtered out by the strict criteria using multiple trajectories.

ACKNOWLEDGMENTS

The authors express their sincere thanks to Richard Swinbank for supplying UKMO assimilation data and trajectory programs, Bjørn M. Knudsen for providing his digital data on diabatic cooling rates, and Hideaki Nakajima and Takafumi Sugita for their excellent comments and suggestions. The data were processed at the ILAS Data Handling Facility, National Institute for Environmental Studies.

REFERENCES

1. P. von der Gathen, et al., Observational evidence for chemical ozone depletion over the Arctic in the winter 1991-92, *Nature*, **375**, pp. 131–134,1995.
2. M. Rex, et al., In-situ measurements of stratospheric ozone depletion rates in the Arctic winter 1991/92: A Lagrangian approach, *J. Geophys. Res.*, **103**, pp. 5843–5853, 1998.
3. M. Rex, et al., Chemical ozone loss in the arctic winter 1994/95 as determined by the Match technique, *J. Atmos. Chem.*, **32**, pp. 35–59, 1999.
4. Y. Sasano, M. Suzuki, T. Yokota, and H. Kanzawa, Improved Limb Atmospheric Spectrometer (ILAS) for stratospheric ozone layer measurements by solar occultation technique, *Geophys. Res. Lett.*, **26**, pp. 197–200, 1999.
5. Y. Sasano, Y. Terao, H. L. Tanaka, T. Yasunari, H. Kanzawa, H. Nakajima, T. Yokota, H. Nakane, S. Hayashida, and N. Saitoh, ILAS observations of chemical ozone loss in the Arctic vortex during early spring 1997, *Geophys. Res. Lett.*, **27**, pp. 213–216, 2000.
6. Y. Terao, H. L. Tanaka, T. Yasunari, and Y. Sasano, ILAS observations of chemical ozone loss and changes in nitric acid and nitrous oxide concentrations in the Arctic vortex during early spring 1997, *Proc. Quadrennial Ozone Symposium Sapporo 2000*, pp. 111–112, 2000
7. E. R. Nash, P. A. Newman, J. E. Rosenfield, and M. R. Schoeberl, An objective determination of the polar vortex using Ertel's potential vorticity, *J. Geophys. Res.*, **101**, pp. 9471–9478, 1996.
8. B. M. Knudsen, et al., Ozone depletion in and below the Arctic vortex for 1997, *Geophys. Res. Lett.*, **25**, pp. 627–630, 1998.
9. A. Schulz, et al., Match observations in the Arctic winter 1996/97: High stratospheric ozone loss rates correlate with low temperatures deep inside the polar vortex, *Geophys. Res. Lett.*, **27**, pp. 205–208, 2000.